WATER RESOURCES RESEARCH, VOL. 18, NO. 6, PAGES 1615–1626, DECEMBER 1982

Settling Velocity of Natural Particles

WILLIAM E. DIETRICH[1]

Department of Geological Sciences and Quaternary Research Center, University of Washington, Seattle, Washington 98195

Data from 14 previous experimental studies were used to develop an empirical equation that accounts for the effects of size, density, shape, and roundness on the settling velocity of natural sediment. This analysis was done in terms of four nondimensional parameters, namely, the dimensionless nominal diameter D_*, the dimensionless settling velocity W_*, the Corey shape factor, and the Powers roundness index. For high D_* (large or dense particles), changes in roundness and shape factor have similar magnitude effects on settling velocity. Roundness varies much less for naturally occuring grains, however, and hence is a less important control than shape. For a typical coarse sand with a Powers roundness of 3.5 and a Corey shape factor of 0.7, the settling velocity is about 0.68 that of a sphere of the same D_*, with shape and roundness effects contributing about equally to the settling velocity reduction. At low D_* the reduction in settling velocity due to either shape or roundness is much less. Moreover, at low D_*, low roundness causes a greater decrease in settling velocity at low shape factor values than at high shape factor values. This appears to be due to the increased surface drag on the flatter grains.

INTRODUCTION

The rate at which a particle settles through a static fluid depends on the density and viscosity of the fluid and on the density, size, shape, roundness, and surface texture of the particle. Although the gross effects of these factors on settling velocity are well known, the functional relationship is, in general, poorly quantified. No theory based on the physics of flow around irregular objects exists to predict the settling velocity of natural particles. In its absence, researchers have proposed empirical curves based on laboratory experiments. Some have attempted to characterize the settling velocity of natural sediment possessing 'typical' properties with a single curve of settling velocity as a function of size [*Rubey*, 1933; *Graf*, 1971; *Baba and Komar*, 1981*a*]. Others have suggested sets of curves that account separately for particle properties affecting settling velocities [*Schultz et al.*, 1954; *Colby*, 1957; *Alger*, 1964; *Alger and Simons*, 1968; *Komar and Reimers*, 1978]. Unfortunately, authors in the second group have tended to work within a limited range of particle and fluid properties and several of them did not control or identify all factors affecting the measured settling velocities, so these curves are of limited utility.

The settling velocity of a particle influences its mode, rate, and distance of transport by shearing forces in a fluid. In addition, the settling of crystals may alter the geochemical evolution of a cooling magma and the eventual mineralogic composition of a rock. In either case, calculation of grain movement requires data on the physical properties and settling velocities of the actual grain of interest. Some workers [e.g., *Gibbs et al.*, 1971] have proposed reporting settling velocities in terms of a 'sedimentation diameter' where the latter is defined as the diameter of a sphere of the same specific gravity and the same terminal uniform settling velocity as the given particle in the same sedimentation fluid [see *Colby*, 1957, p. 14]. This approach, which several authors have endorsed, yields values for grain size or settling velocity that cannot be used properly in calculations of grain movement unless the grain is in fact spherical. Similarly, empirical curves grouping all data on the settling of sand without regard to density and viscosity of the fluid and shape and roundness of the particles are of limited value in sediment transport studies. The graphs and equations presented here, although slightly more complex, use actual particle properties and should help overcome these deficiencies.

In this paper, data from many previous settling velocity experiments are drawn together and through a systematic analysis, an empirical expression is developed. This expression accounts for the effects of size, density, shape, and roundness separately and provides a simple means of predicting the settling velocity of irregularly shaped particles. Data on special geometric objects such as cubes, cylinders, cones, and discs were not included owing to the emphasis on natural sediment. The precision of the final expression is limited by the quality of the available experiments, which is poor in defining the effects of roundness.

CONTROLS ON SETTLING VELOCITY

Dimensionless Forms of Particle Size and Settling Velocity

A particle released in a less dense Newtonian fluid initially will accelerate through the fluid due to its weight. Resistance to deformation of the fluid, transmitted to the particle by the surface drag on it and pressure differences across it, generates forces that act to resist the particle motion. These forces depend on the velocity and the acceleration of the particle. The grain will cease to accelerate and will travel at a constant speed when the gravitational force F_g is exactly balanced by the sum of the two resistant forces, F_D. It is the settling velocity w_s that arises under these conditions that we seek to predict from the physical properties of the fluid and the particles.

The force due to the weight of a particle can be written as

$$F_g = (\rho_s - \rho)gV \tag{1}$$

where ρ_s and ρ are the densities of the grain and fluid, respectively, g is gravitational acceleration, and V is the volume of the particle. The resistant force F_D is

$$F_D = C_D\rho \frac{w_s^2}{2} A \tag{2}$$

where C_D is dimensionless coefficient of drag and A is the cross-sectional area of the particle. The drag coefficient depends

[1] Now at the Department of Geology and Geophysics, University of California at Berkeley, Berkeley, California 94720.

Paper number 2W1332.
0043-1397/82/002W-1332$05.00

TABLE 1. Sources of Data

Particle Type	Source	Number of Points
Smooth spheres	*Alger* [1964]	8
	Allen [1900]	31
	Arnold [1911]	78
	Gibbs et al. [1971]	17
	*Liebster**	14
	*Lunnon**	13
	Pettyjohn and Christiansen [1948]	48
	Stringham et al. [1969]	56
Oblate and prolate ellipsoids	*Stringham et al.* [1969]	78
Ellipsoidal, well-rounded gravel	*Alger* [1964]	64
	Komar and Reimers [1978]	51
	Romanovskiy [1966]	52
Natural sediment	*Briggs et al.* [1962]	128
	Corey† [1949]	46
	Schultz† [1954]	101
	Wilde† [1952]	262
Crushed sediment	*Schultz*† [1954]	58
	Wilde† [1952]	53

* Data obtained from *Rouse* [1938, Figure 94, p. 215]
† Data reported by Schultz et al. [1954].

on the relative magnitude of the inertial and viscous forces, as expressed by the Reynolds number Re:

$$\mathrm{Re} = \frac{w_s B}{\nu}$$

where B is a representative length scale of the particle and ν is the kinematic viscosity of the fluid.

At terminal velocity, F_g equals F_D, and from (1) and (2),

$$C_D = \frac{(\rho_s - \rho)gV}{(\rho w_s^2/2)A} \tag{3}$$

Traditionally, experimental results of settling velocity studies have been used to develop a graph of the dependency of C_D (as computed from (3)) on Re. From such a graph (see *Rouse* [1938, p. 215] for example) it is possible by iteration to compute the settling velocity knowing the particle size or vice versa. For particles other than well-rounded, smooth spheres, however, problems arise in defining A, the cross-sectional area and B, the characteristic length of the grain. It is possible to measure directly the cross-sectional area of a particle by projecting its image on a screen [e.g., *Schultz et al.*, 1954; *Briggs et al.*, 1962] but the characteristic length B must be chosen. A convenient means to compute B is to equate it to the nominal diameter D_n, [*Wadell*, 1932], which is the diameter of a sphere of the same volume V of the particle.

Schultz et al. [1954] showed larger differences in drag coefficient due to shape for a given Re if A was estimated from $(D_n)^2$ rather than the observed projected area. For this reason and because it is much easier to compute A from D_n than to measure it directly, they proposed that it be standard procedure to set A in (3) equal to $(D_n)^2$. *Colby* [1957] subsequently pointed out that it is more consistent to define A as $\pi/4\ D_n^2$ (the cross-sectional area of the equivalent sphere), and he recomputed the results of Schultz et al. using this definition. Equation (3) then becomes

$$C_D = \frac{4(\rho_s - \rho)g\ D_n}{3\rho w_s^2} \tag{4}$$

Definition of A in this manner is useful because variations in shape greatly affect the cross-sectional area of a particle. By computing A as the equivalent cross section of a sphere, effects due to lack of sphericity can be expressed explicitly by a shape factor correction.

Many researchers [e.g., *Rouse*, 1938; *Schultz et al.*, 1954; *Yalin*, 1972] have pointed out that the problem of having to iterate to compute the settling velocity from data expressed in C_D–Re space and the difficulty of defining the cross-sectional area of a particle can be avoided by a simple coordinate transformation. Instead of expressing experimental results in terms of C_D and Re, they can be expressed in terms of a dimensionless settling velocity W_* and dimensionless particle size D_*, defined as

$$W_* = \frac{\rho w_s^3}{(\rho_s - \rho)g\nu} \tag{5}$$

$$D_* = \frac{(\rho_s - \rho)g\ D_n^3}{\rho\nu^2} \tag{6}$$

The dimensionless settling velocity is the inverse of the velocity coefficient C_w proposed by *Wilde* [1952] and *Malaika* [1949], and if V and B are defined in terms of the nominal diameter,

$$W_* = (4/3)\mathrm{Re}/C_D$$

Similarly, the dimensionless particle size D_* is equal to the size coefficient C_s of *Wilde* [1952] and *Malaika* [1949] multiplied by $\pi/6$ and

$$D_* = (3/4)C_D\mathrm{Re}^2$$

Yalin [1972, p. 69] also used the dimensionless particle size D_* to represent the settling velocity of spheres.

Size and Density of Settling Particle

The settling velocity of a smooth sphere as a function of size and density has been studied experimentally and theoretically by numerous authors, and data plotted on C_D–Re graphs are shown in most textbooks on fluid mechanics. Less effort has been devoted to developing a numerical expression fitted to available experimental data. The most widely used such expression in sedimentologic applications is that given by *Gibbs et al.* [1971]. This curve was fitted to 17 data points which were the average of several measurements made by the authors. The large amount of data generated in previous studies by numerous other authors was not included in their analysis, and it was not clear how well their data and expression conformed to these earlier works. Also, the form of the Gibbs et al. equation is sufficiently complex that it could not be converted and expressed in terms of W_* and D_*.

In order to examine the variation of settling velocity as a function of particle size and density alone, data on the settling velocity of smooth spheres (Table 1) were plotted in terms of W_* and D_* (Figure 1). The form of the relation between W_* and D_* is well defined by these 265 data points, and the shape of this curve can be explained in the same manner as given in most fluid mechanics textbooks for the equivalent curve plotted in C_D–Re space. For this reason the form of this curve will only be discussed briefly here.

The dimensionless number D_* is a ratio of the gravitational force acting on the particle to the viscous resistance of the fluid. At low D_*, viscous forces are significant and the magnitude of the drag force on the settling sphere can be computed from theory (Stokes' law). The theoretical solution is

$$F_D = 3\mu\pi D w_s \tag{7}$$

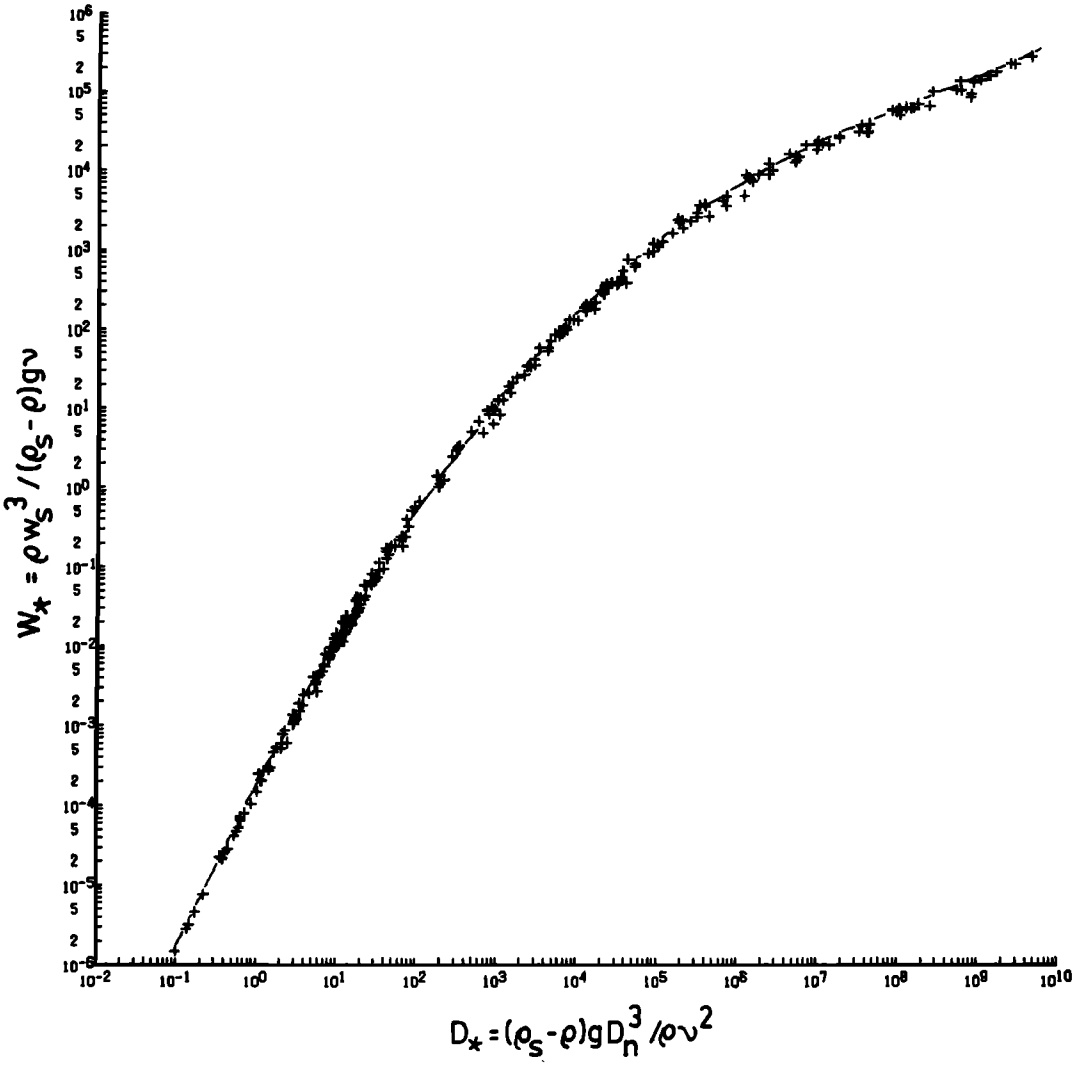

Fig. 1. Settling velocity of spheres plotted as a function of W_* and D_*. Sources of data given in Table 1. Curve is a least squares fit of a fourth order polynomial (equation (9)).

where μ is the dynamic viscosity of the fluid. Setting (7) equal to (1) and converting to dimensionless form yields

$$W_* = \frac{D_*^2}{5832} = 1.71 \times 10^{-4} D_*^2 \quad (8)$$

The trend of the data for D_* less than about 2.0 in Figure 1 has a slope of about 2.0, as predicted by (8). For larger D_*, progressive growth and instability of the flow separation field around the sphere causes the pressure drag to increase more rapidly for a given increase in settling velocity and W_* increases less rapidly with increasing D_*. Once the separation wake is fully turbulent, the pattern of flow distortion around a sphere changes little with increasing D_* and the slope in Figure 1 becomes roughly constant. In this case, C_D is nearly constant; setting F_g equal to F_D yields $W_* \propto D_*^{0.5}$, and the slope of the data for high D_* in Figure 1 is approximately 0.5. At very high D_* the boundary layer around the sphere may become turbulent reducing the flow separation induced pressure drag and causing W_* to increase more rapidly with D_*. The analysis carried out here did not attempt to document this effect.

To isolate just the influence of size and density on settling velocity, separating their effects from that of shape and angularity, I fit a continuous function to the data points plotted in Figure 1. A polynomial was chosen as the simplest regression equation and two conditions were placed on the regression procedure. The equation was constrained to conform to Stokes' law for D_* less than 2.0 by heavily weighting the regression with data generated by (8). The data above D_* of 6×10^8 were not used in the regression. There appears to be a slight kink in the relation between W_* and D_* in this region, yet there is also an increase in scatter of the data and a paucity of data. At approximately 5×10^9 D_* the boundary layer around the sphere be-

TABLE 2. Regression Statistics for Spheres

	Value
N	252
R^2	0.999
S	0.0729
$\%\bar{w}_s$	± 4.9
$\bar{w}_s$	3.0

N is the number of data points, R is the correlation coefficient, S is the standard error of the estimate for five degrees of freedom, and $\%\bar{w}_s$ is the standard error of the estimate as a percentage of the mean settling velocity $\bar{w}_s$ in centimeters per second. Note that regression was done with logarithmic transformed data; S is in log w_* units.

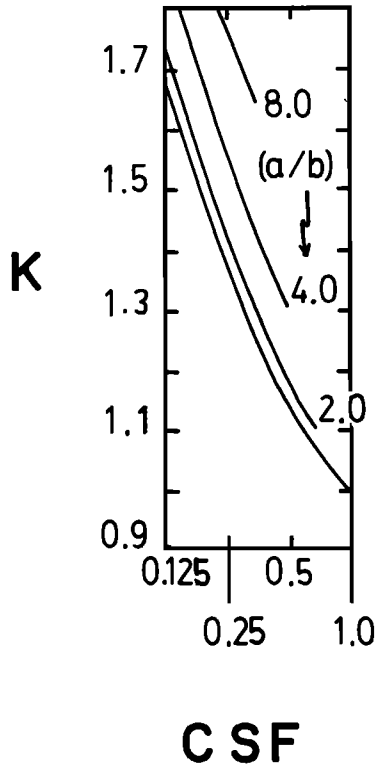

Fig. 2. Correction factor K to Stokes' law predicted for ellipsoids by *McNown and Malaika* [1950]. Axial ratios a/b are given for each curve. Geometric constraints prevent higher values of the Corey shape factor for large values of a/b (Modified from *Graf* [1971]).

comes fully turbulent, causing a reduction in drag and an increase in settling velocity. Rather than increase by several orders the best fit polynomial to the entire data set to account for this upper region, the 13 data points larger than 6×10^8 were not included in the regression. This exclusion lead to an underestimate of the settling velocity by less than 4% for the largest value of D_* observed.

Least squares regression of successively higher order polynomials demonstrated that the residual mean square was not significantly reduced with polynomials higher than fourth order and that the fourth order polynomial fit the data well (Figure 1). The fitted equation is

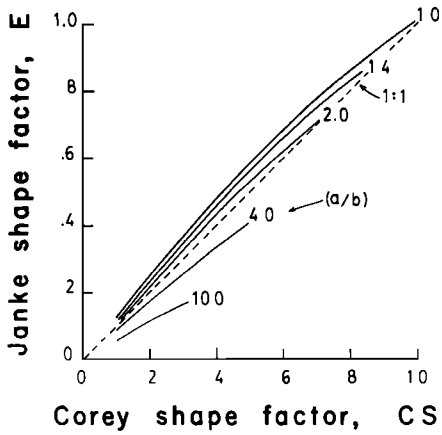

Fig. 3. Relation between Janke shape factor E and the Corey shape factor CSF as controlled by longest to intermediate axial ratios a/b labeled on each curve. Upper limit on line represents geometric constant.

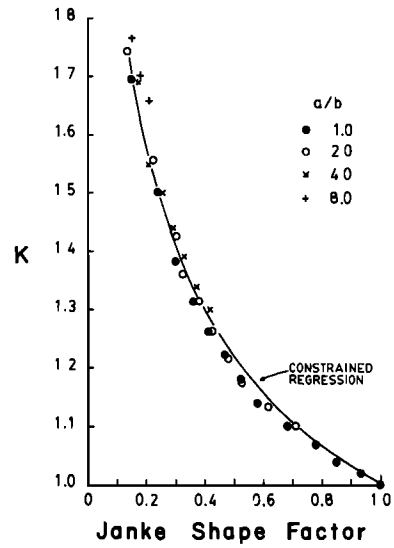

Fig. 4. Digitized curves from Figure 2 expressed as a functions of the Janke shape factor. Curve is a power curve regression constrained to the 1.0 intercept, $R^2 = 0.61$, $N = 33$.

$$\log W_* = -3.76715 + 1.92944(\log D_*) - 0.09815(\log D_*)^{2.0} - 0.00575(\log D_*)^{3.0} + 0.00056(\log D_*)^{4.0} \quad (9)$$

and the regression statistics are given in Table 2. At values of D_* less than 0.05, (9) deviates significantly (greater than 5% for settling velocity w_s) from Stokes' law and (8) should be used. The equation should not be applied to D_* values greater than 5×10^9, as the effects of the development of a turbulent boundary layer around the sphere were not included in this analysis.

Over the range of D_* for which the Gibbs et al. equation was intended to apply (about 1 to 10^6) the settling velocities predicted by their equation and by (9) do not differ by more than about 6% in their estimation of settling velocity. The Gibbs et al. equation gives systematically lower values of settling velocity above a D_* of 10,000, systematically higher values between about 5 and 10,000 and low again below D_* of 5. Although (9) appears to track the data better, these are small differences; the advantages given by (9) are applicability to a longer span of D_* and its usefulness in the subsequent analysis of the effects of shape and roundness.

Shape of Settling Particles

Several aspects of the form of nonspherical particles cause the total drag force F_D to equal the gravitational force on the particle F_g at lower terminal settling velocities than for spheres of equivalent volume. The most stable orientation for irregularly shaped grains is to have their maximum projected area oriented in the direction of fall (see *Middleton and Southard* [1978], among many others, for a discussion). Because of this, when compared with a sphere of the same D_*, the irregularly shaped particle will have a larger surface area around which the fluid must be displaced, and greater pressure and friction drag will develop for the same settling velocity. Deviation from a perfect sphericity will cause grains to have a surface which on parts of the grain are more curved than on a sphere. Large surface curvature, which will tend to border the maximum projected area of the grain, induces flow separation and thereby increases the drag coefficient on the settling particle and reduces the settling velocity for the same D_* as a sphere. Finally,

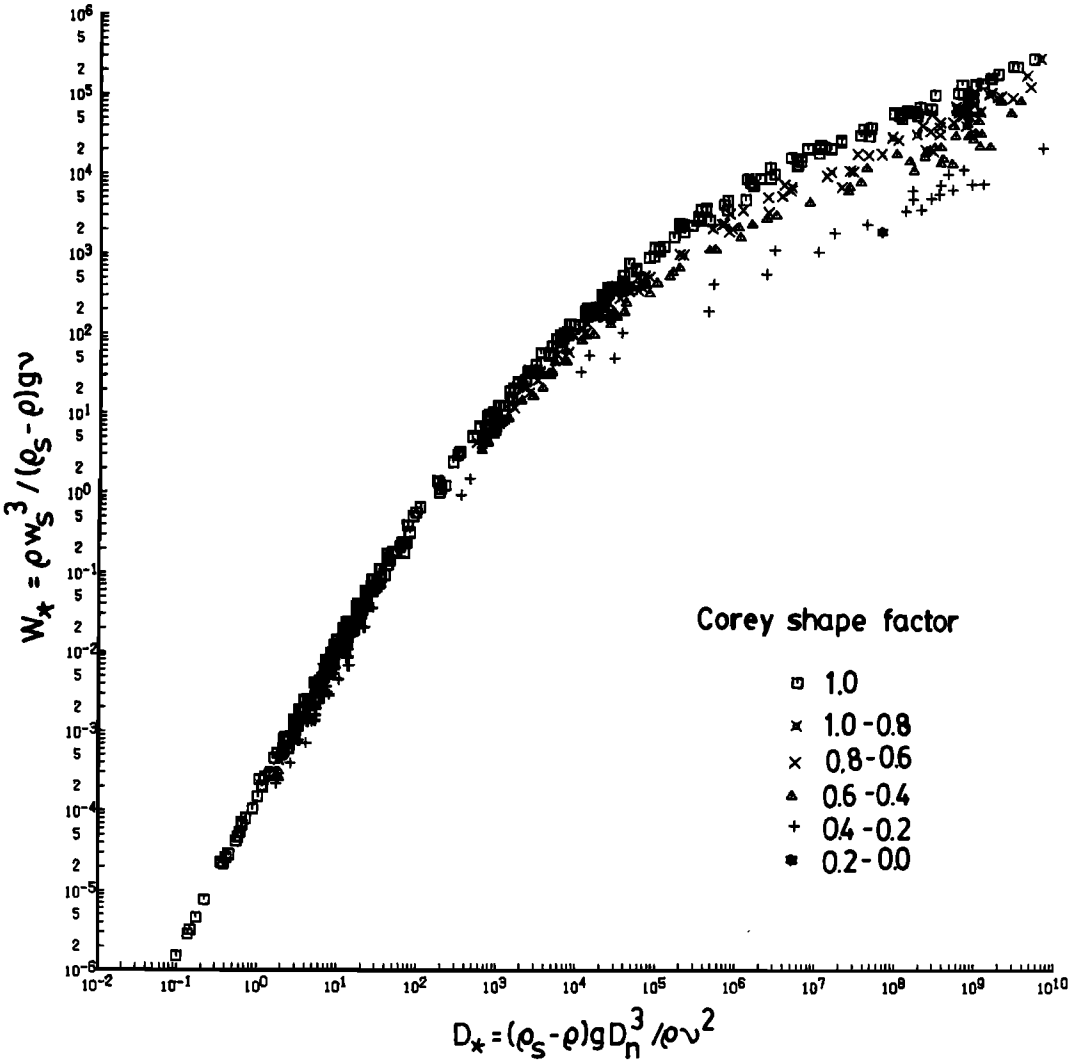

Fig. 5. Settling velocities of well-rounded particles. Data sources given in Table 1.

the shape of the grain may induce an instability in the settling of a particle, which will cause rotation, oscillation, and tumbling that, in general, tends to decrease the vertical settling velocity of the particle (see *Stringham et al.* [1969] or *Middleton and Southard* [1978, pp. 4.6–4.13] for discussion).

Many 'shape factors' have been proposed to characterize the grain shape in a manner that makes estimation of its settling velocity from empirical curves possible. Reviews can be found in the books and papers by *Graf* [1971], *Middleton and Southard* [1978], *Briggs et al.* [1962], *Schultz et al.* [1954], and *Komar* [1980]. A single variable to account for all effects of shape is obviously an oversimplification. Yet in most experimental data currently available, separate effects of shape, roundness, and surface texture were not carefully defined. For practical purposes of prediction of settling velocity based on estimates of size and density of unseen particles, sophisticated shape factors requiring, for example, measurement of particle surface area, seem unwarranted.

Traditionally, the simplest and most commonly used shape factor that has a form which is physically meaningful is the Corey shape factor (CSF) [*Corey*, 1949]:

$$\mathrm{CSF} = \frac{c}{(ab)^{1/2}} \tag{10}$$

where a, b, and c are the longest, intermediate, and shortest axis of the particle, respectively, and are mutually perpendicular. The Corey shape factor, which ranges from greater than zero to 1.0, is a ratio of the cross-sectional area of a sphere to the maximum cross-sectional area of an ellipsoid. The smaller the value of CSF, the flatter the form of the particle. Experimental studies have demonstrated that settling velocities are significantly lower with smaller values of CSF.

McNown and Malaika [1950] have shown that for ellipsoidal particles settling with D_* less than 0.1 (viscous forces dominate), the drag force F_D can be computed from theory and is dependent not only on the Corey shape factor but also on the ratio of longest to intermediate axes (a/b). If Stokes' law is written as

$$F = K\, 3\pi\mu D_n W_s \tag{11}$$

then K is a correction factor controlled by shape. Figure 2 shows the theoretical prediction of K by McNown and Malaika as a function of CSF and (a/b). Clearly there is an a/b dependence in addition to the influence expressed by CSF. Other theories which yield an a/b influence on settling velocity of particles with simple shapes are referenced by *Happle and Brenner* [1965], and *Graf* [1971].

Subsequent to most of the studies of settling velocities of naturally shaped particles, *Janke* [1966] proposed a shape

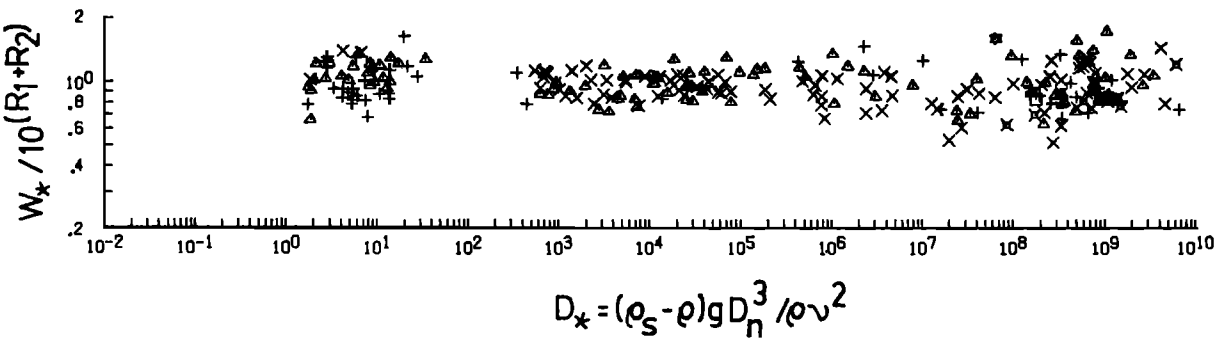

Fig. 6. Residuals of division equation (17) into data for well-rounded natural particles. Symbols are the same as in Figure 5.

factor that required estimates of surface area and angularity. This shape definition has not been adopted because of its complexity and because it has not yet been demonstrated to apply to natural sediment. This definition contains a geometric shape factor term E that is the ratio of the shortest axis of the particle to the root mean square of the three principle axes:

$$E = c\left[\frac{(a^2 + b^2 + c^2)}{3}\right]^{-1/2}$$

Rewriting E in terms of CSF gives

$$E = \mathrm{CSF}\left(\frac{3}{a/b + b/a + \mathrm{CSF}^2}\right)^{1/2} \qquad (12)$$

Equation (12) is shown graphically in Figure 3, where the number labeling each curve is the ratio a/b. Geometric constraints cause progressively smaller maximum ratios of a/b for increasing CSF. For CSF greater than 0.7, there is less than 0.06 variation in E over the range of possible a/b. Note that for a/b equal to about 2.0, the two shape factors are essentially identical in magnitude.

Usefulness of the Janke shape factor can be tested by comparing with the McNown and Malaika theory (It should be noted that Janke intended his shape factor E to be used as a term in a more complete shape measure). This comparison was made by digitizing the curves in Figure 2 and expressing K as a function of E alone, as shown in Figure 4. The Janke shape factor does collapse the data to a single curve which can be expressed as a power function:

$$K = 1.0\, E^{-.28}$$

Setting F_g equal to F_D gives

$$W_s = \frac{1}{18}\frac{1}{\mu}(\rho_s - \rho) g D_n^2\, E^{0.28} \qquad (13)$$

The Janke shape factor, then, is well correlated with a variable that has a theoretical basis. It would appear that in the Stokes range for smooth ellipsoids, the other terms in Janke's general shape parameter are minor contributors.

Equation (13) yields somewhat higher values (up to about 20% greater settling velocity) than the empirical expression of identical form derived by *Komar* [1980] for glass cylinders and ellipsoidal beach gravel. It predicts more closely, however, the experimental results of *Baba and Komar* [1981*b*] on the settling of pieces of 'beach glass' than does the Komar equation. In general, systematic deviations from (13) in experimental results obtained in the Stokes range would suggest that the particles are not perfect ellipsoids and not perfectly smooth.

Outside the realm in which Stokes' law applies the relation between W_* and D_*, as controlled by a shape factor for nonspherical particles, must be derived empirically. Because of its Stokes range correlation with a theoretically based variable, the most correct and reasonably simple shape factor to use would be the Janke shape factor E. This requires, for a given D_* and CSF, data on settling particles for the entire range of possible a/b. These data do not exist because, in part, previous experiments were designed to assess just the dependency of CSF and a range of a/b was not sought. But there is another and, for the purposes of this analysis, more significant reason for the lack of such data. Most naturally occurring grains of interest to the sedimentologist have ratios of a/b that are less than 2.0. This must be true, obviously, for sediment with CSF greater than 0.7 (Figure 3), but it is also true for sediment with smaller values of CSF. The mean CSF for most natural occurring sediment is probably between 0.5 and 0.8, generally decreasing from 0.8 towards 0.5 CSF with decreasing size of sediment in a sample (see examples in the work of *Schultz et al.* [1954, Figure 18, p. 85]). Although the Janke shape factor may be better in principle, in practice the quantification of its role is made difficult by a lack of data in published experiments, and it is made less vital because natural sediment possess a small range in a/b. For these reasons and because the Corey shape factor is the one in current general use, the analysis of the role of shape in controlling settling velocity of particles was done with data on the

TABLE 3. Regression Statistics for Well-Rounded Particles

CSF Class	CSF Mean‡	N	R^2	S^*	$\%\bar{w}_s$	$\bar{w}_s$	R^2†	S†
0.2–0.4	0.30	50	0.999	0.096	±7.3	3.26	0.926	0.836
0.4–0.6	0.50	92	0.999	0.089	6.9	8.89	0.975	0.441
0.6–0.8	0.71	93	0.998	0.079	6.7	24.51	0.975	0.278
0.8–1.0	0.87	8	0.866	0.219	16.9	110.66	0.592	0.378

Symbols as defined in Table 2.
* Standard error of the estimate for six degrees of freedom.
† Regression statistics using just (9) for the same data.
‡ Mean value of shape factor for data in specified class interval.

TABLE 4. Regression Statistics for Grains With Typical Roundness $P = 3.5$

CSF Class	CSF Mean	N	R^2	S^*	$\%\bar{w}_s$	$\bar{w}_s$	R^2†	R^2‡
0.2–0.4	0.33	77	0.982	0.169	13.1	4.47	0.657	0.961
0.4–0.6	0.52	191	0.990	0.140	11.0	7.74	0.838	0.971
0.6–0.8	0.69	227	0.982	0.156	12.0	13.65	0.803	0.926
0.8–1.0	0.84	36	0.980	0.174	13.4	13.88	0.822	0.887
1.0	1.00	6	0.827	0.341	26.1	23.89	0.978	0.987

Symbols as defined in Tables 2 and 3.
* Standard error of the estimate based on seven degrees of freedom, except for 1.00 CSF where it was held to a constant value of 3.
† Regression using (9).
‡ Regression using (17).

Corey shape factor. Future experiments should be designed to define the influence on settling velocity represented by a/b over a large range of D_*.

To isolate just the effects of shape on settling of particles with natural forms, I analyzed data from four studies on the settling of smooth, well-rounded particles. Three of these studies examined the settling of ellipsoidal gravel [*Komar and Reimers*, 1978; *Romanovskiy*, 1966; *Alger*, 1964]. The fourth [*Stringham et al.*, 1969] studied the settling of oblate and prolate spheroids formed from aluminum. Because these spheroids were geometrically similar to smooth, well-rounded natural sediment, they could be included in this analysis. Experimental data on objects with sharp boundaries such as cones, tetrahedrons, and cubes were not included.

Each of the 245 data points derived from these studies was converted into W_* and D_* equivalent values and plotted in Figure 5 along with data on settling of spheres. An expression was then sought of the form

$$W_* = W_*(\text{sphere}) \times f(\text{shape}) \tag{14}$$

Taking the logarithm of (14), and setting $\log f(\text{shape}) \equiv R_2$ yields

$$R_2 = \log W_* - \log W_*(\text{sphere}) \tag{15a}$$

$$R_2 = \log W_* - R_1 \tag{15b}$$

where R_1 equals the right-hand side of (9). As (15*b*) indicates, R_2 is the residual of the logarithm of the observed W_* of a smooth, well-founded particle of any shape and the predicted $\log W_*$ for a sphere of equivalent D_*. A plot of these residuals as a function of D_* for the data shown in Figure 5 revealed that the residuals can be conveniently described by a hyperbolic tangent function centered on D_* of $10^{4.6}$:

$$R_2 = \left(\log\left(1 - \frac{1 - \text{CSF}}{0.85}\right)\right) - (1 - \text{CSF})^{2.3} \tanh(\log D_* - 4.6) + 0.3(0.5 - \text{CSF})(1 - \text{CSF})^{2.0}(\log D_* - 4.6) \tag{16}$$

The first term sets the origin of the hyperbolic function. The second term gives the general form of the residuals, and the third term collapses data at large and small CSF closer toward unity. Because of the form of the first term, (16) cannot be used for CSF less than or equal to 0.15. This is not a major deficiency because so few natural grains possess this shape. The lack of experimental data with low values of CSF suggests that (16) should be used for CSF values greater than 0.2.

Figure 6 gives the final form of the residuals, indicating that there is little remaining structure to the data. The correlation coefficients and other regression statistics are given in Table 3. Addition of the shape factor term greatly reduces the standard error of the estimate and increases the R^2. There is no theoretical justification for the form of (16); it is simply an empirical expression that seems to fit the data well. It does, however, predict the same value of K in (11) for the *Komar and Reimers* [1978] data as is predicted from the McNown-Malaika theory shown in Figure 2.

Rearrangement of (15*b*) gives the following expression for settling velocity for smooth, well-rounded particles of any shape:

$$W_* = 10^{R_1 + R_2} \tag{17}$$

This function can then be divided into the data on settling of particles with natural and artificial roundness and the importance of roundness can be assessed.

Roundness of Settling Particle

The settling of a particle will be influenced by the frequency, magnitude, and distribution of curvature variation along its surface. Distinctions can be drawn between curvature variations that occur over an arc length of less than about 1% of

TABLE 5. Regression Statistics for Crushed Rocks, $P = 2.0$

CSF Class	CSF Mean	N	R^2	S	$\%\bar{w}_s$	$\bar{w}_s$	R^2	R^2	R^2*
0.2–0.4	0.33	26	0.848	0.513	40.5	7.88	0.479	0.866	0.869
0.4–0.6	0.50	42	0.984	0.180	13.9	10.01	0.662	0.935	0.980
0.6–0.8	0.70	36	0.967	0.241	18.5	12.42	0.732	0.883	0.957
0.8–1.0	0.86	7	0.988	0.171	13.2	12.52	0.758	0.883	0.979

Symbols as defined in Table 4.
* Regression using $P = 3.5$ (typical roundness).

TABLE 6. Regression Statistics With Increasing Variables

	Grains With Typical Roundness				Crushed Rocks			
	CSF	S^2	S^2	S^2	S^2	S^2	S^2	S^2
	0.3	0.53	0.06	0.03	0.82	0.22	0.23	0.26
	0.5	0.31	0.06	0.02	0.64	0.13	0.03	0.04
	0.7	0.26	0.10	0.02	0.45	0.20	0.08	0.06
	0.9	0.25	0.16	0.03	0.58	0.28	0.05	0.03
Equation used		(9)	(17)	(19)	(9)	(17)	(19)	(19)
P value				3.5			3.5	2.0

S^2 is residual mean square.

the particle circumference and variations over larger length scales. The smaller length distortions increase the surface drag in the laminar boundary layer for a given settling velocity, thereby increasing the drag coefficient and causing reduced W_* for low values of D_*; the distortions induce turbulence in the boundary layer at very high D_*, causing increased W_* for a given D_* [see *Streeter and Wylie*, 1975, p. 279]. This surface texture effect on settling velocity of natural particles has not been studied. *Williams* [1966] concluded that increased surface texture on spheres and discs only slightly reduced settling velocities. Compared to the effects of shape and larger scale variations, surface texture is probably a very minor influence on settling velocity, and no attempt has been made to quantify it here.

The larger length-scale curvature variations have been grouped under the term 'roundness.' Quantitative definitions have fallen into two categories: measurement of angular deviations from an inscribed circle on the maximum projected area [*Wadell*, 1932; *Wentworth*, 1919] and measurement of the angular deviations from an inscribed circle on a plane parallel to the shortest axis [*Janke*, 1966]. Less precise methods of assigning index numbers of roundness based on comparison with standard images have also been proposed [*Krumbein*, 1941; *Powers*, 1953]. None of these methods account for all aspects of surface curvature variations, and in fact the two quantitative methods measure different but probably equally important aspects of curvature. The most commonly used procedure, the Wadell method, for example, does not distinguish between a disc with sharp edges and a disc with rounded edges, although the latter will settle more rapidly [*Williams*, 1966] because of reduced pressure drag associated with a less pronounced flow separation. Neither method distinguishes between particles with one or several bumps along the projected area. More thorough measures of particle roundness are needed. Perhaps the technique of digitizing projected images parallel to each of the principle axes and doing spectral analyses of the surface curvature may be an improvement [*Ehrlich and Weinberg*, 1970]. This complex analysis, however, requires firm fluid mechanical justification.

Quantitative definition of the role of particle shape developed in the previous section of this paper was derived from data on very smooth particles in which curvature deviations from perfect circles were controlled geometrically by the shape factor. Additional experimental data were grouped into naturally angular sediment and artifically crushed grains (see Table 1 for sources). For most practical purposes the roundness can only be guessed, and the standard method is to assign values of roundness based on a comparison with the images proposed by *Powers* [1953] and the use of *Folk*'s [1955] corresponding numerical scale [see *Blatt et al.*, 1972]. Photographs supplied by *Schultz et al.* [1954] and verbal descriptions by *Briggs et al.* [1962] indicated that a value of 3.5 on a scale of 0.0 (perfectly angular) to 6.0 (perfectly round) was an appropriate Powers roundness value for these naturally shaped grains. The crushed grains were assigned a value of 2.0, and the smooth particles previously analyzed were given a value of 6.0.

To assess just the effect of roundness on settling velocity, I converted the 538 data points from naturally shaped grains into corresponding values of W_* and D_* and divided each measurement by (17). These ratios varied in a manner with D_* that could also be described by the hyperbolic tangent function used in (16). Similar analysis of the ratios of the 111 data points on highly angular crushed grains suggested the following function to account for the residuals controlled by angularity:

$$R_3 = \left[0.65 - \left(\frac{\text{CSF}}{2.83}\tanh(\log D_* - 4.6)\right)\right]^{(1+(3.5-P)/2.5)} \quad (18)$$

where $R_3 = W_*/(10^{R_1+R_2})$ and P is the Powers value of roundness. Note that at $P = 6.0$, (18) equals 1.0, and that at $P = 3.5$, the exponent equals 1.0.

Tables 4 and 5 give the statistics of the fit of (18) to the naturally shaped particles and crushed rocks. Table 6 shows the reduction in residual mean square S^2 by the inclusion of the shape and roundness terms in the prediction of settling velocity. Based on the curvature of the relation between S^2 and the number of variables used, it would seem little more reduction in the residual mean square is possible with the introduction of more terms in the equation. The reduction in S^2 for crushed rocks is less than for the naturally shaped grains because there is a higher variance in the smaller sample set and because the Powers scale is a poor measure of roundness effects. Table 6 also indicates that for CSF greater than 0.5, reduction in residual mean squares occurred by assigning P the value of 2.0 in (18).

Estimation of P is very subjective and as much as ± 1.0 difference in P can be estimated by two observers of the same grain [*Blatt et al.*, 1972]. It would be more useful to develop a more quantitative measure of roundness and to do experiments to demonstrate its value than to try to quantify more exactly the form of the exponent in (16) as controlled by P.

DISCUSSION

The final empirical equation that accounts for size density, shape and roundness of a particle can be written as

$$W_* = R_3 10^{R_1+R_2} \quad (19)$$

where R_1, R_2, and R_3 are the fitted equations for size and density (9), shape (16), and roundness (18), respectively. Figure 7

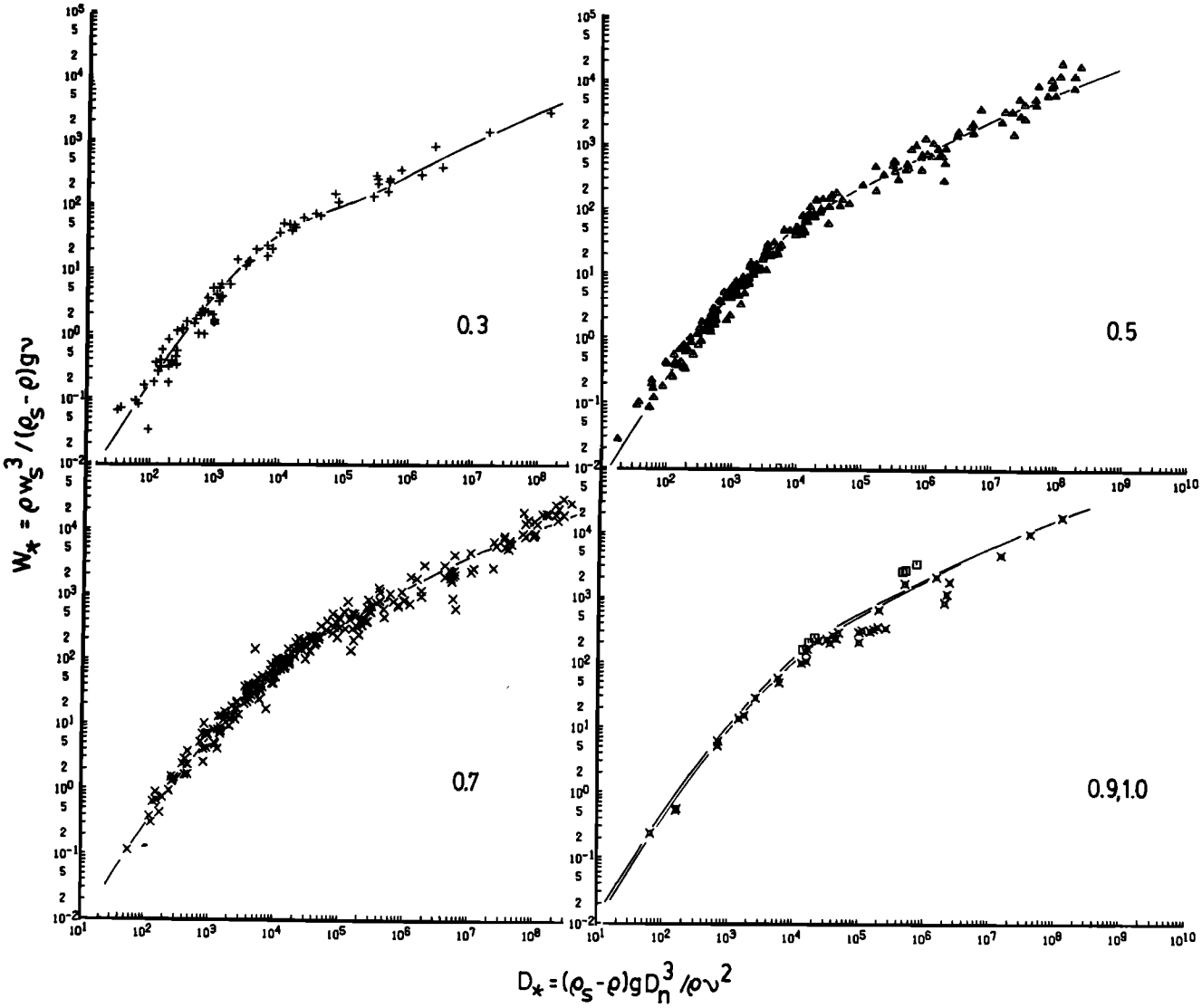

Fig. 7. Comparison between observed and predicted (equation (19)) settling velocity data for naturally rounded grains. Large number in lower right corner of each graph is the Corey factor used in (19). Data on each graph are for particles with CSF values ± 0.1 that are given in left corner. Symbols are the same as in Figure 5.

gives the predicted curves and the measurements for naturally shaped grains. The prediction of the settling velocity for naturally angular but spherical data (CSF = 1.0) is based on eight data points, which are insufficient to define the actual trend of the data with any accuracy. In Figure 8, (19) is depicted graphically for naturally angular ($P = 3.5$) grains. The dominant form of the curve is controlled by size, density, and viscosity, as described previously.

The relative importance of shape and roundness can be examined by selecting a D_* and computing the settling velocity relative to that of a sphere. The form of (19) and the curves in Figure 8 suggest that above a D_* of about 4×10^4 (1.4 mm quartz settling in 20°C water) the effect of shape is roughly the same, that is, the spread between the lines of equal CSF stays relatively constant. A D_* of 1.265×10^5 (2 mm quartz settling in 20°C water) was selected as exemplary of high D_*, and the ratio of settling velocity of particles with $P = 6$, 3.5, and 2 for CSF values of 0.3 and 1.0 were plotted in Figure 9. The presence of the shape factor term in R_3, the roundness term of (19), implies that shape and roundness are interdependent. Clearly, for D_* greater than 4×10^4, distortions on the particle surface will cause much greater reduction in settling velocity if the particle is nearly spherical (CSF = 0.9) than if it is flat (CSF = 0.3) (Figure 9*a*). The decrease in settling velocity of a particle due to shape effects is somewhat less for grains with low roundness. For a typical coarse sand with a Powers roundness of 3.5 and a Corey shape factor of 0.7, the settling velocity is about 0.68 that of a sphere of the same D_* with shape and roundness contributing about equally to the settling velocity reduction. The maximum reduction in settling velocity of a grain with a given roundness due to shape alone is about two-fold. For a grain of a given shape, maximum reduction due to roundness effects is about 1.5 times. Although roundness can be a major control on particle settling velocity, perfectly smooth or crushed grains are rare in the natural environment. For most naturally occurring grains, variation in roundness is small and shape will dominate particle settling velocity.

These conclusions are somewhat different for D_* less than 4×10^4. In Figure 9*b*, reduction in settling velocity caused by shape and roundness are shown for a D_* equal to 1000 (about 0.4 mm quartz falling in 20°C water). The total reduction due to grain irregularities is much less for low D_*: maximum re-

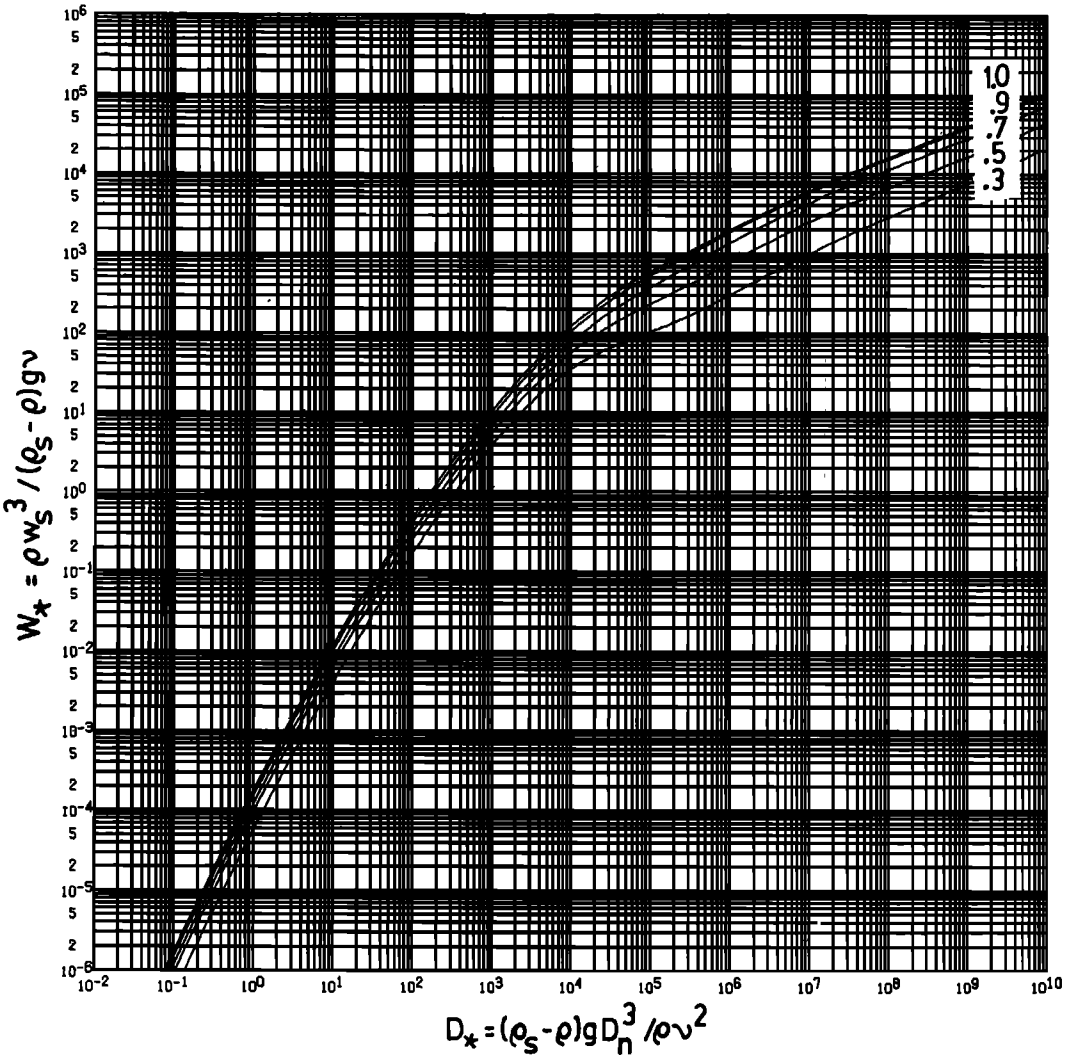

Fig. 8. Empirical curves to predict settling velocity based on (19) for Powers scale equal to 3.5. Numbers on curves are the Corey shape factor. Note that curves for 0.9 and 1.0 CSF nearly merge at large values of D_*.

duction due to shape alone is about 1.5 times; due to roundness alone it is about 1.2 times. Surprisingly, the influence of roundness is apparently greater on flatter grains than on nearly spherical grains. This result suggests that irregularities on a near spherical grain at low D_* cause only slight increases in surface drag in the laminar boundary layer around the grain. The flatter the grain, i.e., the lower the CSF value, the greater the surface area exposed to the fluid. For the same degree of irregularity of that surface (i.e., roundness), greater increases in surface drag may be generated on grains with lower CSF. In contrast, reduction in settling velocity for grains with high D_* comes about principally from pressure drag associated with flow separation. Greater increases in pressure drag can be generated on near-spherical grains than on flat grains for the same high D_*.

Komar and his associates [*Komar and Reimers*, 1978; *Komar*, 1980; *Baba and Komar*, 1981*a*, *b*] have examined several aspects of settling velocity. Recently they have proposed an empirical expression for settling velocity based on the Gibbs et al. equation and a regression based on their experimental data. Their expression is plotted in Figure 10 against a background of the curves for naturally rounded sediment. Their estimate of average P may be closer to 3.0 than 3.5 for their data but is well within observed differences. The Baba-Komar curve is contained within the curves presented here. The range of D_* to which Baba and Komar fit their line follows closely the curve for CSF equal to 0.7. Based on Figure 7 of *Baba and Komar* [1981*a*], it would appear that nearly all of their data fall within the 0.6–0.8 CSF class interval. Outside the range of their data, deviations at high and low D_* from the 0.7 CSF are probably artifacts of the overextention of the limits on the regression. Within the range of their experimental data, their equation for quartz with an average CSF of 0.7 agrees quite well with (19). It is, however, much less general, and it is inaccurate beyond the range of sizes for which it was generated.

Baba and Komar [1981*b*, p. 639] compare their experimental results with the curves shown in Figure 5 of *Komar and Reimers* [1978] and conclude that an as yet unquantified particle character called 'asymmetries' is responsible for 'much of the reduction in settling velocities' from that of perfect spheres, as seen in their data, rather than attributing the reduction to shape and roundness as traditionally defined. It should be pointed out that Figure 5 of Komar and Reimers is entirely wrong and should not be used. In that figure the axes of the

graph are C_D and Re. These axes were defined as

$$C_D = (4/3)(\rho_s - \rho)gD_n/\rho w_s^2$$

$$\mathrm{Re} = w_s D_n/\nu$$

The source of the data plotted on this graph was *Alger*'s [1964] study of the surface area effect on settling of particles of various shapes. Alger proposed a new length, D_a, to be included in a shape factor that was defined as 'the diameter of a sphere having the same surface area as that of the particle' of interest [*Alger and Simons*, 1968, p. 733]. He computed D_a for several particles and plotted his results in a variety of ways but included one [*Alger*, 1964, Figure 14; *Alger and Simons*, 1968, Figure 11] in which

$$C_D = (4/3)\frac{Dn^2}{Da}\frac{(\rho_s - \rho)g}{\rho w_s^2}$$

$$\mathrm{Re} = \frac{w_s D_a}{\nu}$$

It was this figure that was replotted, axes unchanged, as Figure 5 of *Komar and Reimers* [1980]. Thus because D_a is generally much larger than D_n [*Alger and Simon*, 1968, Tables 1, 2, and 4], the points are incorrectly plotted with higher Re and lower C_D by a factor of about 1.3 and 0.78, respectively. This explains in part why the Komar and Reimers curves are poor predictors of the effect of shape: they are plotted in a manner which underestimates the actual drag on the particle. When Alger's data are properly evaluated, it appears that the differences between his smooth particle settling velocities and those of more angular natural sediment can be accounted for as a roundness effect. As suggested previously, the data on roundness are poor, the measurement of it is imprecise, but its importance is undeniable. The effect of asymmetries suggested by *Baba and Komar* [1981*b*], is a valid issue and needs to be included in a better measure of roundness.

Equation (19) is based on an analysis of 1159 data points. For each of these data points there was a varying degree of uncertainty about the correct shape and roundness factor. Also, there were errors generated during measurement of settling velocity that were due both to methodology and particle instability during settling. The division of CSF chosen for the final graphs was that used in standard analyses of shape. The large scatter in the data suggests that except for CSF less than about 0.4, finer categories by shape are unwarranted. In general the 0.9 line was not well defined and the 1.0 is not well established for natural sediment and crushed rock. For general use with typical quartz and feldspar-rich sediments the graph or the equation with P equal to 3.5 and CSF equal to 0.7 is the best estimate of settling velocity.

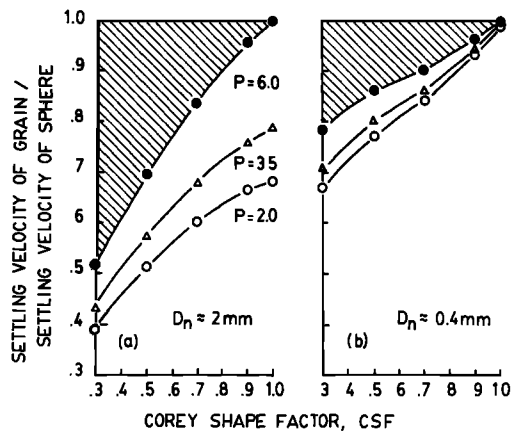

Fig. 9. Reduction in settling velocity from that of a sphere caused by shape and roundness. (*a*) At D_* equal to 1.259×10^5 ($D_n \approx 2$ mm quartz). (*b*) At D_* equal to 1000 ($D_n \approx 0.4$ mm quartz). The shaded region is the reduction in settling velocity due to shape alone.

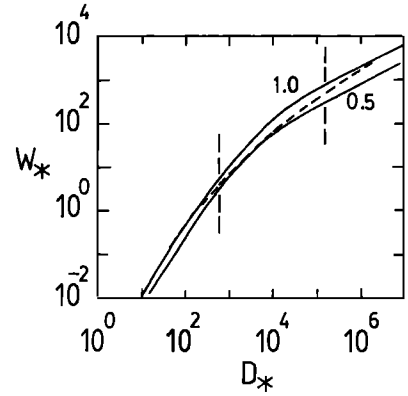

Fig. 10. Comparison of Baba-Komar empirical curve for quartz from an Oregon beach (dashed line) with curves for $P = 3.5$ predicted by (19). Dashed vertical lines indicate the range of D_* to which *Baba and Komar* [1981*a*] fit their curve. The upper and lower curves are for Corey shape factors of 1.0 and 0.5, respectively.

CONCLUSION

Much work on the settling velocities of particles has been done and continues to be done in a manner in which particle properties influencing settling rates are not carefully controlled. Little value can be found in repeated refinement of empirical curves involving these data. It was my intention here to work with the available data to examine and express separately in a quantitative manner the effects on settling velocities of obvious major particle properties. The definitions and the data were imprecise, yet the final expression chosen seems to be a useful way to compute settling velocities based on quantifiable particle properties. By plotting the data as functions of W_* and D_* and including the full range of data available, I have attempted to achieve a generality that goes beyond just the problem of settling of ideal quartz sand in warm water. It is expected that careful examination of the physics of settling of natural particles will lead to more useful, general, and quantitative form factors that are supported by theoretical analysis and from which settling velocities can be more accurately predicted. Such work is a major undertaking. In the interim, it is hoped that the equations and curves presented here may provide a rapid and reasonably accurate procedure to compute settling velocity for naturally shaped particles.

NOTATION

- a longest length axis of a particle.
- A cross-sectional area of a particle.
- b intermediate length axis of a particle.
- B representative length scale in the Reynolds number for a settling particle.
- c shortest length axis of a particle.
- C_D drag coefficient.
- C_s size coefficient.

C_w velocity coefficient.
CSF Corey shape factor, equal to $c/(ab)^{1/2}$.
D diameter of a sphere.
D_a diameter of a sphere having the same surface area as that of the particle.
D_n nominal diameter of a particle.
D_* dimensionless nominal diameter.
E Janke shape factor.
F_g force due to weight of particle.
F_D drag force on settling particle.
g gravitational acceleration.
K correction factor to Stokes law due to shape differing from sphere.
P Powers roundness scale.
R correlation coefficient.
R_1 equation for predicting the settling velocity of spheres.
R_2 equation for predicting the ratio of the settling velocity of a nonspherical, well-rounded particle to be settling velocity of a sphere with the same D_*.
R_3 equation for predicting the ratio of the settling velocity of an angular particle to that of a well-rounded particle.
Re Reynolds number.
S standard error of the estimate.
V volume of a particle.
w_s settling velocity of a particle.
W_* dimensionless settling velocity.
μ dynamic viscosity of the fluid.
ν kinematic viscosity of the fluid.
ρ density of the fluid.
ρ_s density of the particle.

Acknowledgments. J. Dungan Smith encouraged the investigation and suggested many useful revisions of a previous manuscript. Neil Humphrey assisted in some parts of the analysis. Comments by an anonymous reviewer clarified and improved the final manuscript. The study was supported in part by NSF grant ENG 78-16977.

REFERENCES

Alger, G., Terminal fall velocity of particles of irregular shapes as affected by surface area, Ph.D. dissertation, Colo. State Univ., Fort Collins, 1964.

Alger, G., and D. B. Simons, Fall velocity of irregular shaped particles, *J. Hydraul. Div. Am. Soc. Civ. Eng.*, *94*(HY3), 721–737, 1968.

Allen, H. S., The motion of a sphere in a viscous fluid, *Philos. Mag.*, *S.5*(50), 323, 1900.

Arnold, H. D., Limitations imposed by slip and inertial terms upon Stoke's Law for the motion of spheres through liquids, *Philos. Mag.*, *S.6*(22), 755–775, 1911.

Baba, J., and P. D. Komar, Measurements and analysis of settling velocities of natural quartz sand grains, *J. Sediment. Petrol.*, *51*, 631–640, 1981*a*.

Baba, J., and P. D. Komar, Settling velocities of irregular grains at low Reynolds number, *J. Sediment. Petrol.*, *51*, 121–128, 1981*b*.

Blatt, H., G. Middleton, and R. Murray, *Origin of Sedimentary Rocks*, Prentice Hall, Englewood Cliffs, New Jersey, 1972.

Briggs, L. I., D. S. McCulloch, and F. Moser, The hydraulic shape of sand particles, *J. Sediment. Petrol.*, *32*, 645–656, 1962.

Colby, B., Some fundamentals of particle size analysis, Rep. 12, 55 pp., Subcommittee on Sediment., St. Anthony Falls Hydraul. Lab., Minneapolis, Minn., 1957.

Corey, A. T., Influence of shape on the fall velocity of sand grains, MS thesis, Colo. A & M College, Fort Collins, Colo., 1949.

Ehrlich, R., and B. Weinberg, An exact method for characterization of grain shape, *J. Sediment. Petrol.*, *40*, 205–212, 1970.

Folk, R. L., Student operator error in determination of roundness, sphericity and grain size, *J. Sediment. Petrol.*, *25*, 297–301, 1955.

Gibbs, R. J., M. D. Matthews, and D. A. Link, The relationship between sphere size and settling velocity, *J. Sediment. Petrol.*, *44*, 7–18, 1971.

Graf, W. H., *Hydraulics of Sediment Transport*, McGraw-Hill, New York, 1971.

Happel, J., and H. Brenner, Low Reynolds number hydrodynamics, Prentice-Hall, Englewood Cliffs, New Jersey, 1965.

Janke, N. C., Effect of shape upon the settling velocity of regular convex geometric particles, *J. Sediment. Petrol.*, *36*, 370–376, 1966.

Komar, P. D., Settling velocities of circular cylinders at low Reynolds numbers, *J. Geol.*, *88*, 327–336, 1980.

Komar, P. D., and C. E. Reimers, Grain shape effects on settling rates, *J. Geol.*, *86*, 193–209, 1978.

Krumbein, W. C., Measurement and geologic significance of shape and roundness of sedimentary particles, *J. Sediment. Petrol.*, *11*, 64–72, 1941.

Malaika, J., Particle shape and settling velocity, Ph.D. dissertation, State Univ. of Iowa, Ames, 1949.

McNown, J. S., and J. Malaika, Effects of particle shape on settling velocity at low Reynolds numbers, *Eos Trans. AGU*, *31*, 74–81, 1950.

Middleton, G. V., and J. B. Southard, Mechanics of sediment movement, Lecture notes for Short Course 3, 248 pp., Eastern Section of the Soc. of Econ. Paleontol. and Mineralog., Binghampton, N. Y., 1978.

Pettyjohn, E. S., and E. B. Christiansen, Effect of particle shape on free-settling rates of isometric particles, *Chem. Eng. Prog.*, *44*, 157–172, 1948.

Powers, M. C., A new roundness scale for sedimentary particles, *J. Sediment. Petrol.*, *32*, 117–119, 1953.

Romanovskiy, V. V., A study of the fall velocity of coarse sediment, *Sov. Hydrol.*, 47–62, 1966.

Rouse, H., *Fluid Mechanics for Hydraulic Engineers*, Dover, New York, 1938.

Rubey, W., Settling velocities of gravel, sand and silt particles, *Am. J. Sci.*, *225*, 325–339, 1933.

Schultz, E. F., R. H. Wilde, and M. L. Albertson, Influence of shape on the fall velocity of sedimentary particles, *Sediment. Ser. Rep. 5*, 161 pp., Missouri River Div., Corps of Eng., U.S. Army, Omaha, Neb., 1954.

Streeter, U. L., and E. B. Wylie, *Fluid Mechanics*, McGraw-Hill, New York, 1975.

Stringham, G. E., D. B. Simons, and H. P. Guy, The behavior of large particles falling in quiescent liquids, *U.S. Geol. Surv. Prof. Pap. 562-C*, 33 pp., 1969.

Wadell, H., Volume, shape, and roundness of rock-particles, *J. Geol.*, *40*, 443–451, 1932.

Wentworth, C. K., A laboratory and field study of cobble abrasion, *J. Geol.*, *27*, 507–521, 1919.

Wilde, R. H., Effect of shape on the fall-velocity of grand-sized particles, MS thesis, 86 pp., Colo. A & M College, Fort Collins, Colo., 1952.

Williams, G. P., Particle roundness and surface texture effects on fall velocity, *J. Sediment. Petrol.*, *36*, 255–259, 1966.

Yalin, M. S., *Mechanics of Sediment Transport*, Pergamon Press, New York, 1972.

(Received April 23, 1982;
revised August 20, 1982;
accepted August 30, 1982.)